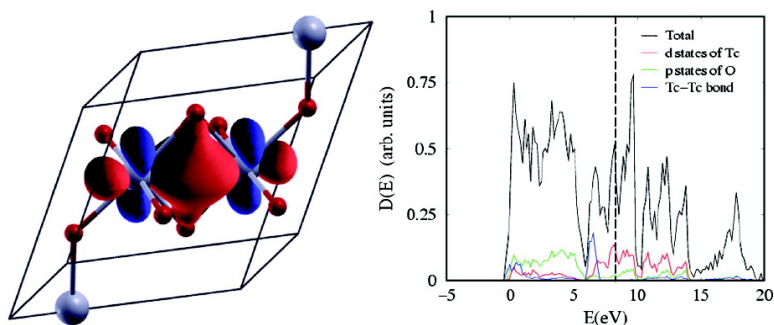


## Structural Studies of TcO by Neutron Powder Diffraction and First-Principles Calculations

Efrain E. Rodriguez, Frederic Poineau, Anna Llobet, Alfred P. Sattelberger, Joydeep Bhattacharjee, Umesh V. Waghmare, Thomas Hartmann, and Anthony K. Cheetham

*J. Am. Chem. Soc.*, **2007**, 129 (33), 10244-10248 • DOI: 10.1021/ja0727363 • Publication Date (Web): 27 July 2007

Downloaded from <http://pubs.acs.org> on February 15, 2009



### More About This Article

Additional resources and features associated with this article are available within the HTML version:

- Supporting Information
- Links to the 5 articles that cite this article, as of the time of this article download
- Access to high resolution figures
- Links to articles and content related to this article
- Copyright permission to reproduce figures and/or text from this article

[View the Full Text HTML](#)

## Structural Studies of TcO<sub>2</sub> by Neutron Powder Diffraction and First-Principles Calculations

Efrain E. Rodriguez,<sup>†,||</sup> Frederic Poineau,<sup>‡</sup> Anna Llobet,<sup>†</sup> Alfred P. Sattelberger,<sup>‡,⊥</sup> Joydeep Bhattacharjee,<sup>§</sup> Umesh V. Waghmare,<sup>§</sup> Thomas Hartmann,<sup>‡</sup> and Anthony K. Cheetham<sup>\*,||</sup>

*Contribution from the Materials Research Laboratory, University of California, Santa Barbara, California 93106-5121, Manuel Lujan Jr. Neutron Scattering Center, Los Alamos National Laboratory, Los Alamos, New Mexico 87545, Harry Reid Center for Environmental Studies, University of Nevada, Las Vegas, Nevada 89154-4009, and Theoretical Sciences Unit, Jawaharlal Nehru Center for Advanced Scientific Research, Jakkur PO, Bangalore 560 064 India*

Received April 19, 2007; E-mail: cheetham@mrl.ucsb.edu

**Abstract:** Crystalline technetium dioxide was prepared and for the first time its crystal structure determined by neutron powder diffraction. In addition, electronic structure calculations using density functional theory were performed to further elucidate the bonding mechanisms in TcO<sub>2</sub>. The crystal structure determined by Rietveld analysis with the NPD data is of a distorted rutile type, similar to that of MoO<sub>2</sub>; space group *P*2<sub>1</sub>/*c*, *a* = 5.6891(1), *b* = 4.7546(1), *c* = 5.5195(1) Å, and  $\beta$  = 121.453(1)°. The NPD analysis also establishes a new neutron scattering length of 6.00(3) fm for <sup>99</sup>Tc. Our results clearly show metal–metal bonding between Tc pairs along the edge-sharing chains of TcO<sub>6</sub> octahedra. The Tc–Tc bond was found to be 2.622(1) Å from NPD profile analysis and 2.59 Å from first-principles DFT calculations. The bond is somewhat longer than expected from earlier predictions, suggesting that the nature of the Tc–Tc interaction is weaker than anticipated for the Tc(IV) cation with three outer electrons. The NPD results supported by the DFT calculations suggest that the filling of antibonding orbitals and the influence of the crystal field stabilization of the d<sup>3</sup> Tc cations lead to more regular TcO<sub>6</sub> octahedra and diminish the metal–metal bond strength compared with closely related oxides such MoO<sub>2</sub> and WO<sub>2</sub>.

### Introduction

No stable isotope of technetium exists but <sup>99</sup>Tc, a pure  $\beta^-$  emitter, is produced in weighable amounts from the nuclear fuel cycle.<sup>1</sup> <sup>99</sup>Tc is a long-lived nuclide with a half-life of  $2.13 \times 10^5$  years and behaves like a true second-row transition metal, its chemistry broadly resembling that of its heavier congener, rhenium.<sup>2,3</sup> Currently, only two oxides of technetium have been unambiguously identified, the light yellow Tc<sub>2</sub>O<sub>7</sub> and the black oxide TcO<sub>2</sub>. The structure of Tc<sub>2</sub>O<sub>7</sub> has been solved, but that of TcO<sub>2</sub> remains unreported. Previous X-ray diffraction (XRD) powder studies have indexed the powder pattern of TcO<sub>2</sub> on the basis of a monoclinic cell with the MoO<sub>2</sub> structure,<sup>4,5</sup> but no refinement of the structure was reported because the Rietveld method was not available at the time of this earlier work.

Through the use of extended X-ray absorption fine structure (EXAFS) spectroscopy, Almahamid et al.<sup>6</sup> were the first to report interatomic distances in TcO<sub>2</sub>. However, the EXAFS work provides information only on the local chemical environment around Tc rather than the atomic coordinates for the structure of the oxide. In the present study, we report for the first time the complete structure of TcO<sub>2</sub> obtained from Rietveld refinement with neutron powder diffraction (NPD) data. Indeed, TcO<sub>2</sub> is the only simple transition metal oxide for which the structure has not been determined. The NPD results provide accurate atomic structural parameters for both the technetium and oxygen and confirm the distorted rutile structure in TcO<sub>2</sub> due to metal–metal bonding as observed in MoO<sub>2</sub> and WO<sub>2</sub>.

Throughout this work we focus on the interesting metal–metal interaction in TcO<sub>2</sub> and compare the NPD results to those of other MO<sub>2</sub> compounds with the distorted rutile structure. Moreover, density functional theory (DFT) calculations were performed to obtain the electronic structure of TcO<sub>2</sub> in order to calculate its structural parameters and further elucidate the nature of the Tc–Tc interaction. Overall, with this structural study of TcO<sub>2</sub> we aim to bring the crystal chemistry of technetium oxides up to date with that of neighboring transition metal oxides and

<sup>||</sup> University of California, Santa Barbara.

<sup>†</sup> Los Alamos National Laboratory.

<sup>‡</sup> University of Nevada.

<sup>§</sup> Jawaharlal Nehru Center for Advanced Scientific Research.

<sup>⊥</sup> Currently at Argonne National Laboratory.

(1) Schwochau, K. *Technetium: Chemistry and Radiopharmaceutical Applications*; Wiley-VCH: Weinheim, Germany, 2000.

(2) Colton, R. *The Chemistry of Rhenium and Technetium*; Interscience Publishers (Wiley): New York, 1965.

(3) Peacock, R. D. *The Chemistry of Technetium and Rhenium*; Elsevier: New York, 1966.

(4) Müller, O.; White, W. B.; Roy, R. *Inorg. Nucl. Chem.* **1964**, *26*, 2075.

(5) Rogers, B.; Shannon, R. D.; Sleight, A. W.; Gillson, J. L. *Inorg. Chem.* **1969**, *8*, 841.

(6) Almahamid, I.; Bryan, J. C.; Bucher, J. J.; Burrell, A. K.; Edelstein, N. M.; Hudson, E. A.; Kaltsoyannis, N.; Lukens, W. W.; Shuh, D. K.; Nitsche, H.; Reich, T. *Inorg. Chem.* **1995**, *34*, 193.

to further explore the materials chemistry and physical properties of technetium oxides.

## Experimental and Computational Methods

**Sample Preparation.** Anhydrous crystalline TcO<sub>2</sub> was prepared by the thermal decomposition of freshly crystallized, white ammonium pertechnetate as described previously.<sup>4,7–9</sup> [Caution: <sup>99</sup>Tc is a weak β<sup>−</sup> emitter ( $E_{\text{max}} = 0.29$  MeV), and extra precautions should be taken when handling it to prevent contamination. All preparations were performed in a fume hood, and a polycarbonate β<sup>−</sup> shield with a thickness of 1 cm was used when manipulating the powders. The cleaning and recrystallization of the pertechnetate salt was performed in a rotation evaporator.] Samples of the salt were then heated in a fused quartz boat to 300–350 °C under flowing argon gas for several hours. The decomposition releases N<sub>2</sub> gas and water. Technetium easily oxidizes to the volatile Tc<sub>2</sub>O<sub>7</sub>, and caution must be taken to avoid heating Tc in air at high temperatures. In order to limit the amount of radioactivity during the preparation, three samples of NH<sub>4</sub>TcO<sub>4</sub> were decomposed separately. The starting samples consisted of approximately 420, 430, and 460 mg of NH<sub>4</sub>TcO<sub>4</sub> and yielded 282, 292, and 300 mg of TcO<sub>2</sub> powder, respectively. The black powders were then heated separately to 700 °C in flowing Ar gas to improve crystallinity. XRD powder patterns of the combined samples could be indexed on the basis of a monoclinic cell with space group P2<sub>1</sub>/c.

**Neutron Powder Diffraction.** Approximately 665 mg of the combined TcO<sub>2</sub> powders were transferred in a glove bag with a helium atmosphere into a vanadium sample holder for the NPD measurements. The NPD patterns were measured on the high-intensity powder diffractometer (HIPD) at the Manuel Lujan Neutron Scattering Center at the Los Alamos Neutron Science Center (LANSCE) between 15 K and room temperature. The neutrons were collected in time-of-flight mode with various detector banks at four different angles covering a *d*-spacing range of 0.4–40 Å. A maximum of 2180 reflections were observed and fit using the GSAS software package.<sup>10</sup>

**Density Functional Theory Calculations.** To determine the structure and nature of bonding independently, we used first-principles calculations<sup>11</sup> of the quantum mechanical ground state of electrons. The calculations were performed using density functional theory (DFT) within the local density approximation (LDA) and a generalized gradient approximation (GGA)<sup>12</sup> to describe the many electron exchange and correlation energies. A standard plane-wave code PWSCF 2.0.1<sup>11</sup> with optimized pseudopotentials<sup>13</sup> was used to represent the interaction between ions and electrons; semicore states of Tc were included in its valence. To obtain a precise picture of the bonding, we used a recently developed approach to construct localized Wannier functions,<sup>14</sup> which are localized in real-space and provide a description of electronic states that readily relate to the nature of the bonding. In the case of metals, normalization of a Wannier function (in this scheme<sup>14</sup>) corresponding to a given bond relates to its bond order. Further details and typical input parameters of these calculations are given in Supporting Information.

## Results

**Neutron Powder Diffraction.** Starting with the known structure of MoO<sub>2</sub>,<sup>15</sup> the Rietveld refinement of the TcO<sub>2</sub>

**Table 1.** Atomic Coordinates and Thermal Parameters for TcO<sub>2</sub> from NPD Results and Coordinates Obtained from the DFT Calculations (LDA and GGA, Respectively), Shown in Italics for Comparison

site	<i>x</i>	<i>y</i>	<i>z</i>	<i>U</i> <sub>iso</sub> (Å <sup>2</sup> )
Tc	0.2621(1)	1.0073(3)	−0.0156(2)	0.0009(1)
	<i>0.266</i>	<i>1.005</i>	<i>−0.014</i>	
	<i>0.265</i>	<i>1.005</i>	<i>−0.015</i>	
O 1	0.1037(2)	0.1883(2)	0.1950(2)	0.0047(2)
	<i>0.105</i>	<i>0.190</i>	<i>0.191</i>	
	<i>0.106</i>	<i>0.189</i>	<i>0.193</i>	
O 2	0.3919(2)	0.7085(2)	0.2704(2)	0.0040(2)
	<i>0.394</i>	<i>0.712</i>	<i>0.270</i>	
	<i>0.392</i>	<i>0.712</i>	<i>0.268</i>	

structure converged to the structural parameters given in Table 1. The structure was fitted to the NPD data with a final residual  $R_{\text{wp}}$  of 2.31% and a  $\chi^2$  of 2.486. Observed and calculated NPD profiles are shown in Figure 1, along with the difference curve and Bragg peak marks. Lattice parameters at room temperature were found to be  $a = 5.6891(1)$ ,  $b = 4.7546(1)$ ,  $c = 5.5195(1)$  Å, and  $\beta = 121.453(1)^\circ$ . For comparison, the values reported by Rogers et al. are  $a = 5.55(1)$ ,  $b = 4.85(1)$ ,  $c = 5.62(1)$  Å, and  $\beta = 121.9(1)^\circ$ .<sup>5</sup> As expected from NPD analysis, accurate values for both the Tc and O structural parameters were obtained. The main interatomic distances are given in Table 2. No structural phase transition was observed between room temperature and 15 K. Slight contraction of the lattice and a decrease of thermal parameters were observed at lower temperatures [ $a = 5.6862(1)$ ,  $b = 4.7518(1)$ ,  $c = 5.5160(1)$  Å, and  $\beta = 121.466(1)^\circ$  at 15 K], and changes in the nearest Tc–Tc distance were small [2.615(1) Å at 15 K].

Preliminary Rietveld analysis of the NPD data showed an occupancy of 0.883(4) for Tc. However, energy dispersive X-ray spectroscopy (EDS) and Rietveld refinement of X-ray powder data on the same sample indicate a Tc:O ratio of 1:2. Therefore, we attribute this result to a discrepancy in the neutron scattering length of <sup>99</sup>Tc. The neutron scattering length of <sup>99</sup>Tc used in the preliminary Rietveld analysis was 6.8 fm, the value listed in a standard table of neutron scattering lengths and cross-sections.<sup>16</sup> In the final refinement we fixed the stoichiometry at TcO<sub>2</sub> and obtained a new value for the neutron scattering length of <sup>99</sup>Tc to be 6.00(3) from NPD analysis. Further NPD experiments on a mixed Tc oxide have confirmed this result.

**Electronic Structure.** As is commonly done in DFT studies of oxides, the atomic structural parameters of TcO<sub>2</sub> were determined while keeping the lattice constants fixed at their experimental values. While the LDA calculations yield a compressive stress on the unit cell consistent with typical underestimation of the lattice constants, the GGA calculations resulted in almost vanishing stresses at the experimental structure. With two distinct choices of initial structures, the structural optimization resulted in the same minimum energy structure. Remarkably, the structural parameters obtained from the energy minimization agree very well with those obtained from the NPD Rietveld refinement (Table 1). Average Tc–Tc bond lengths for first and second neighbors determined with DFT calculations are 2.59 and 3.11 Å, while the average Tc–O bond-length is 1.98 Å. The theoretical value of the Tc–Tc bond-length is slightly smaller than the experimental values indicating

- (7) Vinogradov, I. V.; Konaren, M. I.; Zaitseva, L. L.; Shepelihov, S. V. *Russian J. Inorg. Chem.* **1978**, *23* (7), 977.  
 (8) Sptsyn, V. I.; Kugina, A. F.; Oblava, A. A.; Shakh, G. E.; Govush, A. A.; Belyaeva, L. I. *Russian J. Inorg. Chem.* **1978**, *23* (4), 484.  
 (9) Burnett, B.; Campbell, A. B.; Jobe, D. J.; Lemire, R. J.; Taylor, P. *Radiochim. Acta* **1995**, *69*, 241.  
 (10) Larson, A. C.; Von Dreele, R. B. *General Structure Analysis System (GSAS)*, Los Alamos National Laboratory Report, LAUR 86-748, 2004.  
 (11) Baroni, S.; Corso, A. D.; Gironcoli, S.; Giannozzi, P. <http://www.pwscf.org>.  
 (12) Perdew, J. P.; Burke, K.; Ernzerhof, M. *Phys. Rev. Lett.* **1998**, *80*, 891.  
 (13) Rappe, A. M.; Rabe, K. M.; Kaxiras E.; Joannopoulos, J. D. *Phys. Rev. B* **1990**, *41*, 1227.  
 (14) Bhattacharjee J.; Waghmare, U. V. *Phys. Rev. B* **2006**, *73*, R121102.  
 (15) Magneli A.; Andersson, G. *Acta Chem. Scand.* **1955**, *9*, 1378.

- (16) Dianoux A.-J.; Lander, G. *Neutron Data Booklet*; OCP Science: Institut Laue-Langevin, 2003.

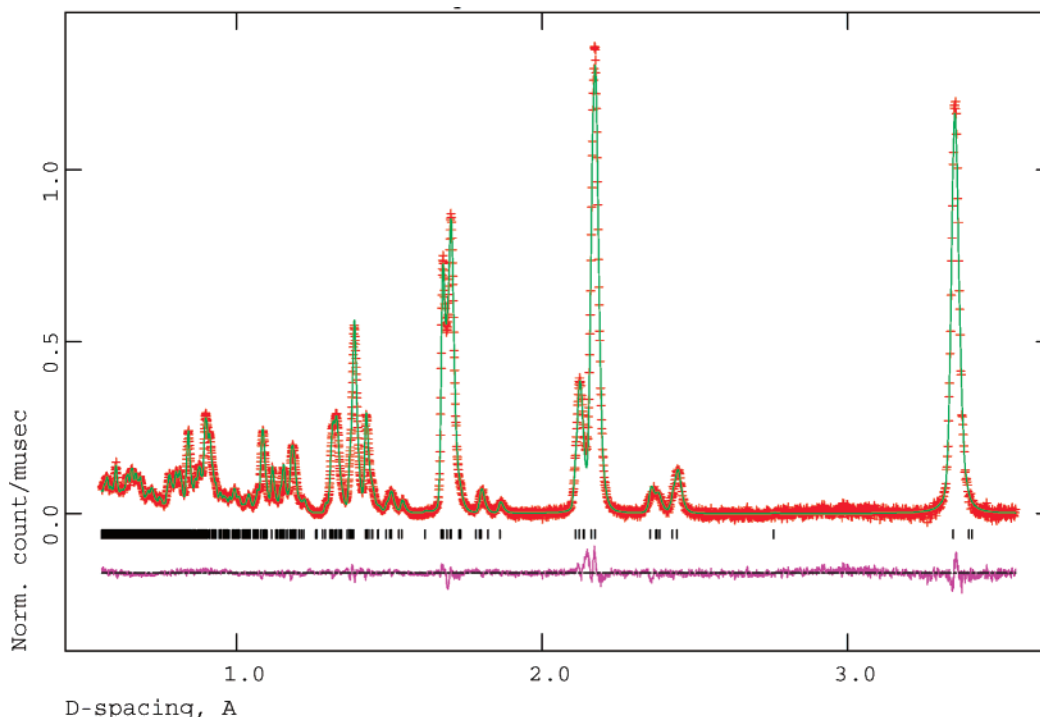


**Figure 1.** The observed (red crosses) and calculated (smooth line) neutron powder diffraction profiles for  $\text{TcO}_2$  with the difference profile (in purple) shown below the powder patterns.

**Table 2.** Interatomic Distances ( $\text{\AA}$ ) in  $\text{TcO}_2$  from the NPD and DFT (LDA) Results

interatomic distance	NPD results ( $\text{\AA}$ )	DFT calculations ( $\text{\AA}$ )	EXAFS ( $\text{\AA}$ ) from ref 6
Tc–Tc	2.622(1)	2.586	2.61
Tc–Tc	3.076(1)	3.110	3.10
Tc–O	1.999(1)	1.994	1.98
Tc–O	2.007(1)	2.029	1.98
Tc–O	1.989(2)	2.009	1.98
Tc–O	1.960(2)	1.933	1.98
Tc–O	1.960(1)	1.951	1.98
Tc–O	1.976(1)	1.980	1.98

that our calculations may give a slight over-binding between the nearest neighbor Tc atoms. Overall, the interatomic distances from the DFT results agree very well with the estimates obtained from the NPD results (Table 2). The total and partial density of electronic states and the Fermi energy position were also calculated for  $\text{TcO}_2$  (Figure 2). The DOS can be separated into three sections: (i) the bands from 0 to 6 eV are primarily made of oxygen p-orbitals, (ii) the bands from 6 to 14 eV are dominated by the technetium 4d orbitals, and (iii) the bands above 15 eV have the character of valence s-electrons of Tc. Although no electrical resistivity measurements have been performed on  $\text{TcO}_2$ , the calculations clearly predict metallic behavior in  $\text{TcO}_2$  with the Fermi level located approximately halfway through the “ $t_{2g}$ ” band. Indeed, structurally related  $\text{MoO}_2$  and  $\text{WO}_2$  have been found to be metallic with room-temperature resistivities of  $0.9 \times 10^{-4}$  and  $3 \times 10^{-3}$  ohm-cm, respectively.<sup>5</sup> In the theoretical work by Eyert et al., the electronic structure calculations for  $\text{MoO}_2$  show a total and partial DOS with similar features as that of  $\text{TcO}_2$  but with the Fermi level at a lower energy in the “ $t_{2g}$ ” band.<sup>17</sup> The DOS

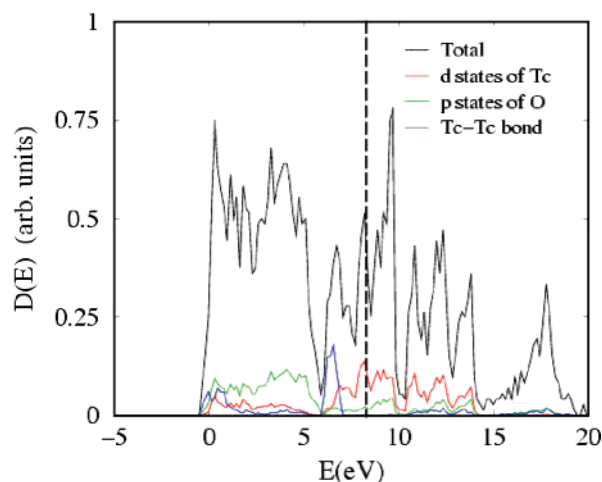


**Figure 2.** Total and partial density of electronic states of  $\text{TcO}_2$  in the neighborhood of the Fermi energy indicated with a dashed line.

will be used to further explain the nature of the metal–metal bond in  $\text{TcO}_2$ .

## Discussion

The resulting structure of  $\text{TcO}_2$  can be described as that of a distorted rutile with Tc–Tc pairing. In the undistorted rutile structure of  $\text{TiO}_2$ ,  $\text{TiO}_6$  octahedra form chains along [001] direction through edge-sharing (Figure 3).<sup>18,19</sup> The chains are cross-linked by shared corners so that the chains are mutually connected to form a three-dimensional structure. The metal atoms are equidistant in the chain while the  $\text{MO}_6$  octahedron is tetragonally distorted so that it is either apically elongated or compressed. The rutile structure type can become distorted if

(18) Bolzan, A. A.; Fong, C.; Kennedy, B. J.; Howard, C. J. *Acta Crystallogr. B* **1997**, *53*, 373.

(19) Wells, A. F. *Structural Inorganic Chemistry*, 5th ed.; Oxford University Press: New York, 1984; Chapter 12.

(17) Eyert, V.; Horny, R.; Hock, K.-H.; Horn, S. J. *Phys.: Condens. Matter* **2000**, *12*, 4923.

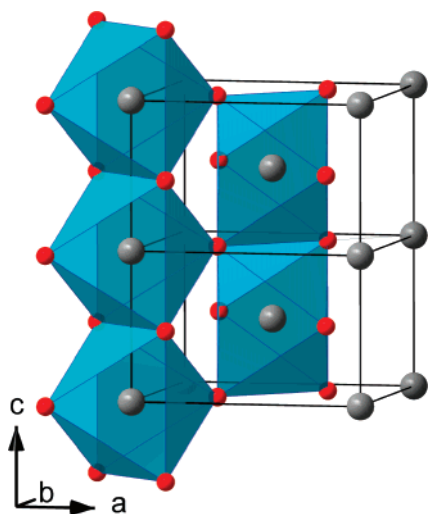


**Figure 3.** Two unit cells of the rutile structure showing the chains of edge-sharing MO<sub>6</sub> octahedra.

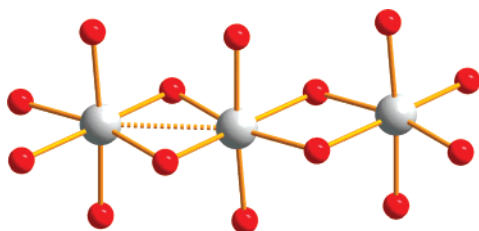


**Figure 4.** A structural unit in TcO<sub>2</sub> consisting of three edge-sharing TcO<sub>6</sub> octahedra. The metal–metal bond is labeled by the dashed line.

the metal cations have one or more valence electrons available for metal–metal bonding. In NbO<sub>2</sub>, for example, a structural change accompanies a metal-to-semiconductor transition at 1070 K when Nb–Nb pairing takes place to form a superstructure based on the rutile structure.<sup>20</sup> Other distorted rutiles adopt the MoO<sub>2</sub> structure, in which successive pairs of metal atoms within the chains become alternately closer together and further apart. For example, the low-temperature VO<sub>2</sub> phase and WO<sub>2</sub> have the MoO<sub>2</sub> structure with metal–metal bonding.<sup>21,22</sup> The NPD results show that TcO<sub>2</sub> adopts the MoO<sub>2</sub> structure with Tc–Tc distances that are alternately 2.622(1) and 3.076(1) Å, which agree quite well with the Tc–Tc distances obtained from the EXAFS study by Almahamid et al. (Table 2). It should be noted that the EXAFS assumes that all the Tc–O bond lengths in the TcO<sub>6</sub> octahedra are equal, which, of course, is not the case. Figure 4 shows the main structural element of TcO<sub>2</sub> consisting of three edge sharing octahedra within the chain.

It is interesting to compare the results from our NPD study with the corresponding data for the other metal oxides with distorted rutile structures (Table 3). MnO<sub>2</sub>, which is undistorted, is shown for comparison. In an early study of dioxides with the MoO<sub>2</sub> structure, Magneli and Andersson<sup>15</sup> proposed that the

Tc–Tc metal bond should be as short as 2.48 Å based on the assumption that the Tc atom positions were equal to those of Mo in MoO<sub>2</sub>. Likewise, in an extensive study of metal oxides with rutile and rutile-derived structures, Rogers et al.<sup>5</sup> predicted that TcO<sub>2</sub> would have a much stronger Tc–Tc interaction than is found in the present work. In their study, the metal–metal bonds in VO<sub>2</sub> and NbO<sub>2</sub> are 2.65 and 2.75 Å, respectively, whereas for MoO<sub>2</sub> and WO<sub>2</sub> a shorter bond with a distance of 2.50 Å is found. Rogers et al. concluded that the metal–metal bond is a first-order bond for the V and Nb pairs and a second-order bond for Mo and W. Similarly, they proposed the bond would be of higher order in TcO<sub>2</sub> than in VO<sub>2</sub> and NbO<sub>2</sub>. However, the NPD results from the present study reveal a longer bond between the Tc cations than was suggested in these early studies. In fact, our experimental and theoretical findings are more consistent with the early phenomenological treatment of Goodenough<sup>23</sup> and the early theoretical work of Burdett.<sup>24</sup>

It is also possible to infer the strength of the metal–metal interaction from the axial ratio  $c/a$ .<sup>21</sup> From Figure 3 one can observe how the octahedron can become either apically compressed or elongated by simply noting the axial ratio of the tetragonal cell. As the metal–metal interaction increases, the  $c/a$  ratio decreases. For the monoclinic cell, the  $c/a$  ratio was taken to be  $a/(b + c \sin \beta)$ .<sup>5</sup> The  $c/a$  ratios for several distorted rutiles and MnO<sub>2</sub> are collected in Table 3. The study by Rogers et al. predicted TcO<sub>2</sub> to have the lowest  $c/a$  ratio in the series of MO<sub>2</sub> compounds based on the assumption that it would form the strongest metal–metal bond in the series. However, our NPD results show that this is not the case as the  $c/a$  ratio for TcO<sub>2</sub> was found to be intermediate between those of VO<sub>2</sub>/NbO<sub>2</sub> and MoO<sub>2</sub>/WO<sub>2</sub>. Thus, it again appears that in TcO<sub>2</sub> the metal–metal bond is closer to first order.

Manganese and rhenium are in the same column as technetium, but comparing the bonding mechanisms in TcO<sub>2</sub> to those in MnO<sub>2</sub> and ReO<sub>2</sub> can be ambiguous since TcO<sub>2</sub> is the only one with the MoO<sub>2</sub>-type structure and alternating M–M distances. MnO<sub>2</sub> adopts the regular rutile structure<sup>5,19</sup> and ReO<sub>2</sub> is polymorphic, with  $\alpha$ -ReO<sub>2</sub> having the MoO<sub>2</sub> structure and  $\beta$ -ReO<sub>2</sub> having an orthorhombic structure. Unlike the other distorted rutiles,  $\beta$ -ReO<sub>2</sub> adopts a unique structure in which the edge-sharing octahedra form zigzag chains rather than straight chains.<sup>25,26</sup> Only the  $\beta$ -ReO<sub>2</sub> has been structurally characterized, and it is believed that  $\alpha$ -ReO<sub>2</sub> is a low-temperature phase that converts irreversibly above 300 °C to the zigzag chains in order to permit the formation of short Re–Re distances of 2.61 Å instead of alternate short and long M–M distances as seen in TcO<sub>2</sub> (Figure 4).<sup>15,25</sup> Nevertheless, the Re–Re distance in  $\beta$ -ReO<sub>2</sub> of 2.61 Å is very similar to that seen in TcO<sub>2</sub> (2.622 Å).

The electronic structure of TcO<sub>2</sub> was analyzed to probe the metal–metal bonding further. Examining each of the Wannier functions that describe occupied subspace of electronic states,

**Table 3.** Data on the Metal–Metal Interactions in Some Metal Dioxides with Rutile-Derived Structures

compound	lattice type	outer electron configuration	M–M distances (Å)	$c/a$ ratio	references
VO <sub>2</sub>	monoclinic	3d <sup>1</sup>	2.66; 3.13	0.635	5, 22
NbO <sub>2</sub>	body-centered tetragonal	4d <sup>1</sup>	2.74(2); 3.26(2)	0.6176(1)	20
MoO <sub>2</sub>	monoclinic	4d <sup>2</sup>	2.508(3); 3.114(3)	0.5790(4)	21
WO <sub>2</sub>	monoclinic	5d <sup>2</sup>	2.496(3); 3.091(3)	0.5708(2)	21
MnO <sub>2</sub>	tetragonal	3d <sup>3</sup>	2.87	0.653	5
TcO <sub>2</sub>	monoclinic	4d <sup>3</sup>	2.622(1); 3.076(1)	0.6012(2)	this work
ReO <sub>2</sub>	orthorhombic	5d <sup>3</sup>	2.61	–	25

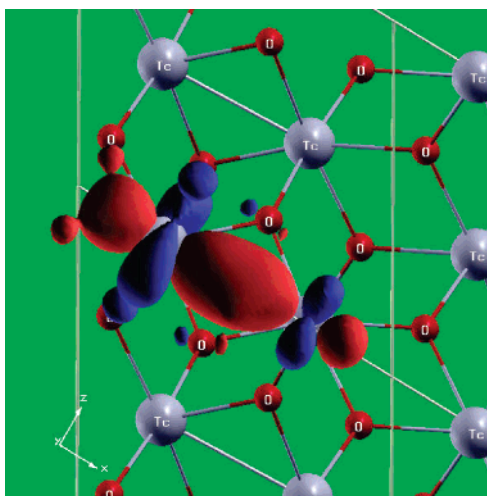


**Figure 5.** Iso-surface of a Wannier function (at 0.005 au) that represents bonding between Tc atoms centered at the edge-sharing octahedra. Red and blue colors represent positive and negative values of the Wannier function, respectively.

the one with d-orbital character of Tc describes the Tc–Tc bond (Figure 5); it arises from a d orbital of the “ $t_{2g}$ ” type. The Tc d-states are significantly split due to the low symmetry of the structure and have a rather large bandwidth (though it is usually overestimated in LDA calculations). The participation of the “ $t_{2g}$ ” orbital in the metal–metal bond is consistent with other theoretical investigations of metal oxides with the rutile structure, distorted or undistorted.<sup>23,24</sup> At low amplitudes this Wannier function also exhibits a weak component of p-orbitals of oxygen, revealing the multicentricity of this bond. (Figure 5) Based on the normalization of this Wannier function, the estimated bond order of the Tc–Tc bond is 0.9, consistent with the interpretation of present experimental results. Wannier functions with the character of other d-orbitals of Tc reflect bonding between Tc and O (Figure 6). As evident in the total and partial density of electronic states (Figure 2), the width of the p-bands of oxygen is about 6 eV, slightly larger than that in the perovskite oxides. These bands also have noticeable contribution from the d-orbitals of Tc, reflecting strong p-d hybridization. The density of states projected onto the Wannier function corresponding to the Tc–Tc bond (Figure 2) confirms its partial occupation and also a weak component of p-states of oxygen in it. It is also noted that the Tc–Tc bond does not contribute to the metallic behavior of  $\text{TcO}_2$ .

It is interesting to ask why the metal–metal bond in  $\text{TcO}_2$  is significantly longer than the corresponding distance in  $\text{MoO}_2$  and  $\text{WO}_2$  (Table 3). We believe that this difference stems from the stronger ligand field stabilization energy associated with the  $t_{2g}^3$  configuration of  $\text{Tc}^{4+}$  compared with the  $t_{2g}^2$  configuration of  $\text{Mo}^{4+}$  and  $\text{W}^{4+}$ . This leads to  $\text{TcO}_6$  octahedra that are more regular than the  $\text{MO}_6$  octahedra found in  $\text{MoO}_2$  and  $\text{WO}_2$ ; specifically, the Tc–O bond lengths in  $\text{TcO}_2$  span a narrow range from 1.96 to 2.01 Å, whereas those in both  $\text{MoO}_2$  and  $\text{WO}_2$  vary between 1.97 and 2.08 Å.<sup>21</sup> It seems probable that

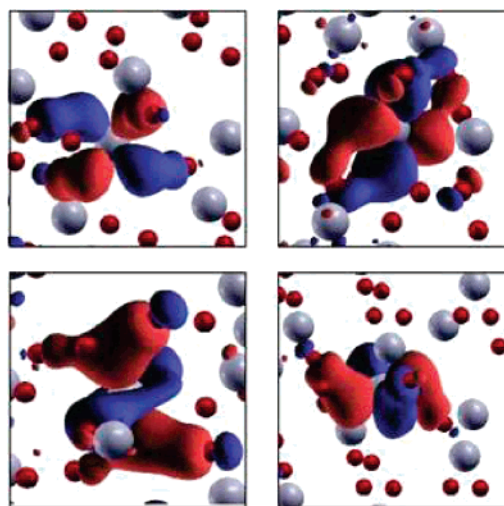


**Figure 6.** Iso-surfaces of Wannier functions that represent bonding between Tc and O atoms involving p-states of oxygen and d-states of Tc. Red and blue colors represent positive and negative values of the Wannier function, respectively.

the short M–M bond lengths in  $\text{MoO}_2$  and  $\text{WO}_2$  are formed at the expense of distorting these octahedra (Figure 4).

## Conclusions

In summary, we have determined for the first time the crystal structure of  $\text{TcO}_2$  by neutron powder diffraction and the interatomic distances obtained from the NPD results show a Tc–Tc bond length of 2.622(1) Å. The Tc–Tc bond length is longer than anticipated from earlier predictions and the metal–metal interaction therefore weaker than predicted by these early studies of metal dioxides with rutile-type structures.<sup>5,15</sup> In addition, first-principles calculations support the NPD results on the strength of the Tc–Tc interaction and show through the use of the localized Wannier function that the bond is composed mostly of Tc “ $t_{2g}$ ” type d-states. Furthermore, the total and partial density of states from the DFT calculations show that the rest of the d-states of the  $\text{Tc(IV)}$  cations do not participate further in metal–metal bonding but fill an M–O  $\pi^*$  band, as had been predicted by the early theoretical work of Goodenough.<sup>23</sup> This filling of the M–O  $\pi^*$  band increases the crystal field stabilization of  $\text{Tc(IV)}$  cations, creates more regular  $\text{TcO}_6$  octahedra as confirmed from the NPD results, and weakens the metal–metal interaction compared with the closely related oxides  $\text{MoO}_2$  and  $\text{WO}_2$ .

**Acknowledgment.** We are grateful to Carol J. Burns from Los Alamos National Laboratory for supplying us with the pertechnetate salt, the starting material for all our technetium chemistry and thank Steve D. Conradson for fruitful discussions. Also, this work has benefited from the use of HIPD at the Lujan Center at the Los Alamos Neutron Science Center, funded by DOE Office of Basic Energy Sciences. Los Alamos National Laboratory is operated by Los Alamos National Security LLC under DOE Contract DE-AC52-06NA25396.

**Supporting Information Available:** Complete ref 27. Further details and input parameters for the DFT calculations. Crystallographic information file. This material is available free of charge via the Internet at <http://pubs.acs.org>.

JA0727363

- (20) Cheetham A. K.; Rao, C. N. R. *Acta Crystallogr. B* **1976**, *32* (part 5), 1579.  
 (21) Bolzan, A. A.; Kennedy, B. J.; Howard, C. J. *Austral. J. Chem.* **1995**, *48*, 1473.  
 (22) Goodenough, J. B. *J. Solid State Chem.* **1971**, *3*, 490.  
 (23) Goodenough, J. B. *Prog. Solid State Chem.* **1971**, *5*, 145.  
 (24) Burdett, J. K. *Inorg. Chem.* **1985**, *24*, 2244.  
 (25) Magneli, A. *Acta Chem. Scand.* **1957**, *11*, 28.  
 (26) Magneli, A. *Acta Crystallogr.* **1956**, *9*, 1038.  
 (27) Gonze, X.; et al. *Comput. Mater. Sci.* **2002**, *25*, 478.